JEE Journal of Ecological Engineering

Journal of Ecological Engineering, 2026, 27(10), 72–85
https://doi.org/10.12911/22998993/224181
ISSN 2299–8993, License CC-BY 4.0

Received: 2026.04.29
Accepted: 2026.07.04
Published: 2026.09.01

Synthesis and characterization of silica-potassium adsorbent by palm oil boiler ash for enhanced carbon dioxide adsorption

Renita Manurung[1*], Taslim[1], Okta Bani[1], Sri Zahrani Dwi Mauliyah Parinduri[1], Norhayati Abdullah[2], Muhammad Faisal Padang[1], Theresia Ivana Sinuraya[1], Muhammad Rizki Ramadan N[1]

[1] Department of Chemical Engineering, Faculty of Engineering, Universitas Sumatera Utara, Medan 20155, Indonesia
[2] Faculty of Chemical and Process Engineering Technology, Universiti Malaysia Pahang Al-Sultan Abdullah, Lebuh Persiaran Tun Khalil, 26300 Kuantan, Pahang Malaysia
* Corresponding author: renita.manurung@usu.ac.id

ABSTRACT

Carbon dioxide (CO_2) capture is increasingly important for mitigating greenhouse gas emissions and reducing environmental impacts associated with fossil fuel utilization. Although palm oil mill boiler ash has been extensively studied for heavy metal adsorption, its application as a CO_2 adsorbent remains limited. Meanwhile, the accumulation of boiler ash waste presents a major environmental challenge for the palm oil industry due to the increasing volume of solid waste generated annually. Therefore, this study investigates the potential utilization of palm oil mill boiler ash as a sustainable silica-based adsorbent for CO_2 capture. The study involved silica synthesis, KOH impregnation, and CO_2 adsorption evaluation. The effects of citric acid concentration (1–5 wt.%), KOH concentration (1–5 M), and impregnation temperature (60–90 °C) on the physicochemical properties and adsorption performance of the adsorbent were systematically investigated. The synthesized materials were characterized using SEM–EDX, FTIR, BET, and XRD analyses to evaluate their morphology, elemental composition, pore structure, and crystallinity. The results showed that silica synthesized using 4% citric acid achieved the highest silica purity of 95.6%, with crystalline phases dominated by cristobalite and tridymite structures. Subsequent impregnation with 5 M KOH significantly enhanced the adsorption performance, resulting in a maximum CO_2 adsorption capacity of 144.8 mg/g at an impregnation temperature of 80 °C. Kinetic analysis revealed that the adsorption process followed a pseudo-second-order model, indicating that chemisorption was the dominant adsorption mechanism. Palm oil mill boiler ash-derived silica adsorbents possess promising potential as sustainable and low-cost materials for CO_2 capture applications.

Keyword: carbon-dioxide capture, impregnation, palm oil boiler ash, potassium adsorbent, silica.

INTRODUCTION

Rapid industrialization and sustained population growth have been key drivers of economic development over recent decades, but they have also intensified environmental pressures, particularly through the continuous rise in atmospheric carbon dioxide (CO_2) emissions. In Indonesia, the energy and forestry sectors represent the largest sources of greenhouse gas emissions, primarily due to fossil fuel combustion, deforestation, and land-use change. The increasing reliance on coal and petroleum-based fuels to support industrial production, electricity generation, and transportation has substantially amplified the national carbon footprint. This trend is further exacerbated by rising per capita income and population growth, which continue to stimulate energy consumption and transportation demand. Similar emission trajectories have been reported in several rapidly developing Asian economies, including China, India, the Republic of Korea, Malaysia, Pakistan,

Sri Lanka, and Thailand. Long-term projections indicate that Indonesia's CO_2 emissions will continue to increase through 2050, with coal remaining the dominant contributor due to its extensive utilization in power generation, particularly on Java Island (Cahyono et al., 2022).

Globally, the combustion of fossil fuels, including coal, oil, and natural gas, accounts for nearly 45% of anthropogenic CO_2 emissions (Sattari et al., 2021; Sathishkumar & Prakash, 2026). The continued expansion of fossil fuel consumption has resulted in unprecedented atmospheric CO_2 accumulation, leading to deteriorating air quality, intensified greenhouse effects, and accelerated climate change. Consequently, mitigating CO_2 emissions has become one of the most critical environmental priorities, given its dominant role in global warming and long-term climate instability (Dziejarski et al., 2023; Putri et al., 2026).

Recognizing the urgency of this challenge, the Intergovernmental Panel on Climate Change (IPCC) has emphasized the need for immediate and substantial emission reduction measures. According to the IPCC 2022 assessment report, global greenhouse gas emissions must peak before 2025 and decline by approximately 43% by 2030 to limit severe climate impacts. Failure to achieve these targets could result in an increase in global average temperature of up to 3.2 °C and atmospheric CO_2 concentrations approaching 570 ppm by the end of the century (Gunawardene et al., 2022). In response, considerable efforts have been directed toward the development of low-carbon technologies, including renewable energy systems, biofuels, and gasification processes. Nevertheless, carbon capture and storage (CCS) has emerged as one of the most promising and strategically important technologies due to its ability to directly mitigate CO_2 emissions from large-scale industrial and energy-related sources (Ajiz et al., 2025; Francy et al., 2025).

Carbon capture and storage (CCS) has emerged as a key mitigation technology for reducing anthropogenic CO_2 emissions by enabling the capture and long-term sequestration of carbon from large-scale industrial and energy-intensive processes. Despite its considerable potential, several technical challenges continue to limit its widespread implementation. One notable issue is the formation and accumulation of solid CO_2 on heat exchanger surfaces during the capture cycle, which can impair heat transfer performance and consequently reduce overall process efficiency (Sattari et al., 2021; Kupgan et al., 2018). To address these limitations, adsorption-based CO_2 capture has attracted increasing attention owing to its operational simplicity, energy efficiency, and favorable mass transfer characteristics. The high surface area, well-developed pore structure, and low diffusion resistance of porous solid adsorbents facilitate rapid CO_2 transport and adsorption, thereby enhancing capture performance. In addition, solid adsorbents exhibit superior chemical and thermal stability and are generally less prone to corrosion than conventional liquid absorbents, making them particularly attractive for long-term industrial applications (Penchah et al., 2020). Consequently, substantial research efforts have been devoted to the development of advanced adsorbent materials, including metal–organic frameworks (MOFs), zeolites, alkali-based sorbents such as K_2CO_3, and activated carbon, all of which have demonstrated considerable potential for improving CO_2 adsorption capacity and selectivity (Hui et al., 2025; Dias et al., 2026; Cho et al., 2026).

Palm oil mill boiler ash, a by-product generated from the combustion of palm kernel shells and fibers, has attracted increasing attention as a low-cost precursor for adsorbent development due to its high silica (SiO_2) and alumina (Al_2O_3) contents. These oxides provide abundant surface hydroxyl groups (Si–OH and Al–OH) and porous structures that can serve as active sites for gas adsorption and subsequent surface functionalization. However, the direct utilization of raw palm oil mill boiler ash is often hindered by the presence of inorganic impurities, including metal oxides and mineral residues, which can block pore structures, reduce accessible surface area, and limit the availability of active adsorption sites. Therefore, an effective purification step is essential to enhance the physicochemical properties of the material prior to its application as a CO_2 adsorbent.

Among various purification agents, citric acid offers several advantages due to its environmentally benign nature, biodegradability, and strong metal-chelating capability. The treatment with citric acid facilitates the removal of undesirable metallic impurities while preserving the silica-rich framework, thereby exposing a greater number of silanol groups and improving pore accessibility. According to Manurung et al. (2023), the use of citric acid as a purification agent achieved

a silica recovery yield of 95.9%, demonstrating its effectiveness in removing impurities while preserving the silica-rich structure. Nevertheless, although purification can improve surface cleanliness and porosity, the intrinsic affinity of silica-rich materials toward CO_2 remains relatively limited because of the weak interaction between the adsorbent surface and acidic CO_2 molecules. To overcome this limitation, alkaline impregnation using potassium hydroxide (KOH) has been widely recognized as an effective surface modification strategy. KOH is frequently selected because of its ability to generate a more reactive surface and a more open pore structure, particularly in silicate-based systems. The interaction between KOH and silica-rich materials promotes pore development, increases specific surface area, and introduces additional basic sites that enhance the adsorption of acidic CO_2 molecules through acid–base interactions. Furthermore, the incorporation of potassium-containing species on the adsorbent surface can improve CO_2 affinity and adsorption capacity, making the material more suitable for carbon capture applications (Tumurbaatar et al., 2023).

Although several studies have investigated the use of industrial by-products and porous materials for CO_2 capture, significant research gaps remain. Misran et al. (2019) evaluated coal ash as a CO_2 adsorbent, while Sylvia et al. (2021) reported a relatively low adsorption capacity of only 0.35 mg g^{-1} for untreated palm oil mill boiler ash. Other studies have focused on commercial adsorbents, such as zeolite 5A (Boonchuay and Worathanakul, 2022) and activated carbon (Mohammad et al., 2020), which generally exhibit superior adsorption performance but often require costly raw materials and energy-intensive preparation processes. Based on the available literature, systematic investigations on the combined effects of citric acid purification and KOH impregnation on silica-rich palm oil mill boiler ash for CO_2 adsorption remain scarce. Therefore, this study aims to develop a value-added CO_2 adsorbent from palm oil mill boiler ash through sequential purification and alkaline impregnation treatments. The proposed approach is expected not only to enhance the physicochemical properties and adsorption performance of the material but also to provide a sustainable pathway for the valorization of palm oil industry waste while contributing to carbon emission mitigation.

MATERIAL AND METHODS

Material

The palm oil boiler ash used in this study was sourced from a mill located in Deli Serdang, North Sumatra, Indonesia. This ash is a by-product of the combustion of oil palm mesocarp fiber at temperatures ranging from 700 to 800°C. It consists primarily of a fine powder with particle sizes not exceeding 0.074 mm. For the experimental procedures, analytical-grade citric acid (Merck), KOH pellets (99 wt%, Merck), deionized water, distilled water, and high-purity CO_2 (99.995%) were utilized.

Method

Silica synthesis

A schematic illustration of the research methodology is presented in Figure 1. Citric acid solutions with concentrations ranging from 1–5% were prepared by dissolving citric acid in distilled water. Subsequently, 20 g of palm oil boiler ash was added to 500 mL of the prepared solution and stirred using a magnetic stirrer at 70 °C for 60 min. The resulting mixture was then washed thoroughly with distilled water to remove residual acid and subsequently filtered. The obtained solid was oven-dried at 60 °C for 60 min, followed by calcination at 700 °C for 3 h to obtain purified silica (SiO_2). The morphology and elemental composition of the synthesized silica were characterized using Scanning Electron Microscopy

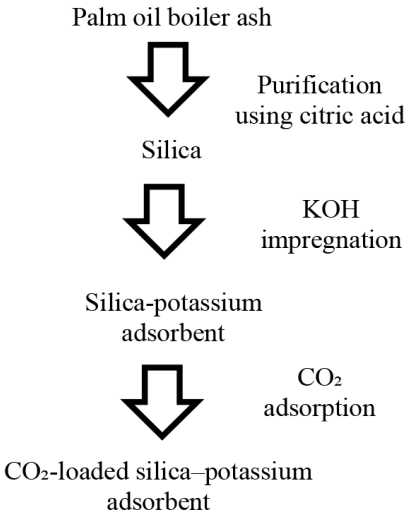

Figure 1. Schematic CO_2 adsorption using silica-potassium adsorbent

coupled with Energy-Dispersive X-ray spectroscopy (SEM–EDX) and X-ray Diffraction (XRD).

Synthesis of silica-potassium adsorbent

Potassium hydroxide (KOH) solutions with concentrations ranging from 1–5 M were prepared in distilled water. Purified silica derived from palm oil ash was subsequently added to the KOH solution at a ratio of 20 g per 1000 mL. The mixture was stirred under reflux conditions at temperatures between 50 and 90 °C for 4 h to facilitate the impregnation process. After impregnation, the suspension was filtered and oven-dried prior to calcination at 700 °C for 3 h. The resulting silica–potassium adsorbent was characterized using Scanning Electron Microscopy–Energy Dispersive X-ray spectroscopy (SEM–EDX) and Fourier Transform Infrared Spectroscopy (FTIR) to evaluate its surface morphology, elemental composition, and functional groups. The silica–potassium adsorbent exhibiting the best adsorption performance was selected for Brunauer–Emmett–Teller (BET) analysis to evaluate its specific surface area and pore properties.

Adsorbent characterization

The synthesized silica and silica–potassium adsorbent were comprehensively characterized using several analytical techniques. Surface morphology and elemental composition were evaluated using a Hitachi S-3400N Scanning Electron Microscope coupled with Energy-Dispersive X-ray spectroscopy (SEM–EDX). The crystalline phases of the adsorbent were identified using an Aeris Benchtop X-ray Diffraction (XRD) instrument. Functional group analysis was performed using Fourier Transform Infrared Spectroscopy (FTIR, Nicolet iS5, Thermo Scientific) over a wavenumber range of 400–4000 cm^{-1}. Furthermore, the specific surface area and pore properties of the adsorbent were determined based on the Brunauer–Emmett–Teller (BET) method using a Micromeritics ASAP 2020 V4.02 analyzer.

CO_2 adsorption

The adsorption experiment was initiated by accurately weighing the adsorbent sample before introducing it into a stainless-steel adsorption column (8 cm outer diameter and 20 cm height). In the first stage (vacuuming process), both the adsorption and reference columns were evacuated to the desired vacuum pressure to remove residual gases and moisture from the system. After the evacuation process, the inlet valve of the adsorption column was closed, and the initial pressures of both columns were recorded (presented in Figure 2 and Table 1).

In the second stage (gas filling process), the reference column was pressurized with CO_2 gas to 500 kPa, followed by closure of the inlet valve to maintain a constant pressure condition. Subsequently, in the third stage (adsorption process), the valve connecting the reference column to the adsorption column was opened to initiate CO_2 adsorption, while pressure variations were monitored at 10 s intervals. Pressure data were continuously recorded until adsorption equilibrium was achieved, as indicated by five consecutive stable pressure readings.

Upon completion of the adsorption process, the remaining gas was safely released through the outlet valve. The adsorbent was then removed

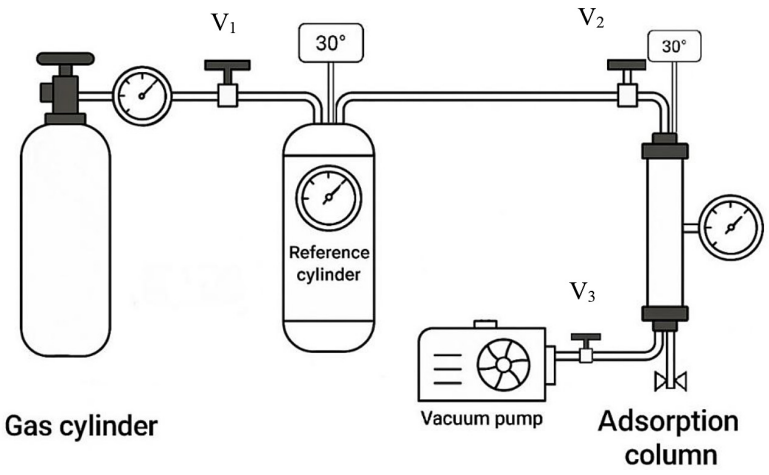

Figure 2. CO_2 adsorption experiment set up

Table 1. The conditions for each operating procedure

Procedure	V_1	V_2	V_3	Additional operation	Stop condition
Vacuuming	Close	Open	Open	Vacuum pump was turned on	Duration reached 15 min
Gas filling	Open	Close	Close	CO_2 was released	T_1 pressure reached 500 kPa
Adsorption	Close	Open	Close	Pressure and temperature were recorded every 10 second	Data did not change for 5 consecutive records

from the column, and its final mass was measured and recorded for subsequent adsorption capacity analysis.

RESULT AND DISCUSSION

Elemental composition analysis

In this study, silica was synthesized from palm oil boiler ash using citric acid solutions with concentrations ranging from 1–5%. The influence of citric acid concentration on the elemental composition of the synthesized silica was evaluated using Energy Dispersive X-ray (EDX) analysis. The results are presented in Table 2.

The EDX results demonstrate that citric acid concentration significantly influences the purity and elemental composition of the synthesized silica. Silicon (Si) was identified as the dominant element in all samples, indicating the successful extraction and purification of silica from palm oil boiler ash. The Si content increased progressively with increasing citric acid concentration, reaching a maximum value of 95.6% at 4 % citric acid, before slightly decreasing to 94.6% at 5%. This trend suggests that citric acid effectively removed inorganic impurities and enriched the silica content of the material. The enhanced silica purity can be attributed to the chelating ability of citric acid, which promotes the dissolution and removal of metallic impurities from the ash matrix (Umeda & Kondoh, 2010).

In contrast, magnesium (Mg) and calcium (Ca) were detected as residual impurities originating from the combustion ash. The concentrations of these elements generally decreased after citric acid treatment, indicating that the purification process successfully reduced the presence of metal oxides and mineral residues. Citric acid acts as a complexing agent capable of forming stable chelate complexes with divalent metal ions such as Mg^{2+} and Ca^{2+}, facilitating their removal during the washing and filtration stages (Wardhani et al., 2017). However, fluctuations in Mg and Ca concentrations were observed at higher acid concentrations. For example, the Mg content decreased from 1.3% at 1% citric acid to 0.7% at 2%, but subsequently increased to 1.8% at 5 %. Similarly, the Ca concentration decreased from 5.1% to 1.9% at 4% citric acid before increasing again at 5 %.

These fluctuations may be associated with re-adsorption or re-precipitation of dissolved metal species onto the silica surface at excessive acid concentrations. In addition, overly aggressive acid treatment may partially alter the silica framework, thereby affect the stability of the porous structure and promote the retention of residual metal species (Fouda-Mbanga et al., 2024; de Castro-Alves et al., 2024). The presence of CaO and MgO impurities is undesirable because these compounds can block pore channels, reduce specific surface area, and negatively affect adsorption performance. Furthermore, Mg species may react with silica to form magnesium silicate phases, which can reduce silica purity and interfere with the formation of an amorphous silica structure favorable for adsorption applications.

As illustrated in Figure 3, the increase in Si content observed at moderate citric acid concentrations indicates that the purification process enhanced the accessibility of silica-rich phases by removing associated impurities. However, the

Table 2. Elemental composition of silica synthesized using different citric acid concentrations

Compound	1%	2%	3%	4%	5%
Mg	1.3	0.7	1.3	1.2	1.8
Si	93.4	93.3	94.0	95.6	94.6
Ca	5.1	2.6	3.0	1.9	2.5
Others	0.2	3.4	1.7	1.3	1.1

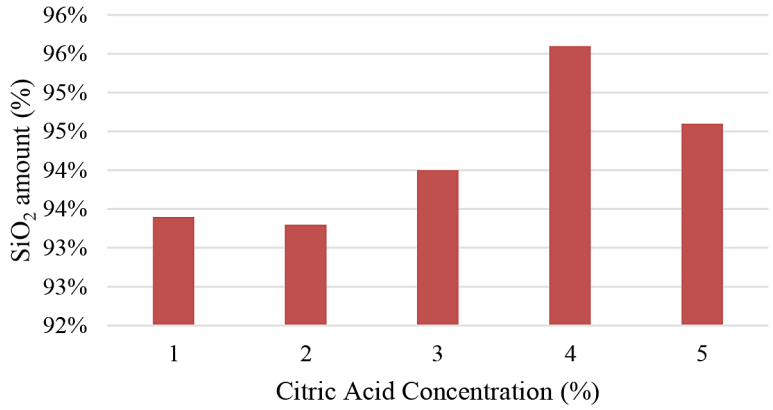

Figure 3. Effect of citric acid concentration on the elemental composition and purity of synthesized silica

slight decline in Si content at 5 % citric acid suggests that excessive acid concentration may induce partial dissolution of the Si–O–Si network, resulting in structural degradation of the silica framework (Li et al., 2025). Therefore, the balance between impurity removal and silica structural stability plays a critical role in determining the optimal purification condition.

Overall, the results indicate that 4% citric acid produced the highest silica purity with the lowest residual impurity content, suggesting that this concentration represents the optimum purification condition for silica synthesis from palm oil boiler ash. Consequently, the silica obtained under this condition was selected for subsequent KOH impregnation and further CO_2 adsorption studies

Silica synthesized from palm oil boiler ash exhibited the highest silica purity at a citric acid concentration of 4 wt.%, achieving a Si content of 95.67%. The purified silica was subsequently subjected to potassium hydroxide (KOH) impregnation to enhance the adsorption performance of the adsorbent by increasing surface basicity and active adsorption sites. KOH impregnation was carried out using five different concentrations, namely 1, 2, 3, 4, and 5 M. The elemental composition of the resulting silica–potassium adsorbents, particularly the K_2O content, was analyzed using Energy Dispersive X-ray (EDX) spectroscopy. The compound compositions of the adsorbents obtained at different KOH concentrations are presented in Table 3.

The EDX analysis demonstrated that KOH impregnation significantly influenced the elemental composition and structural characteristics of the silica-based adsorbent. The major components detected in the adsorbent included SiO_2, K_2O, MgO, CaO, and Al_2O_3, whose concentrations varied considerably with increasing KOH concentration. Among all samples, the highest SiO_2 content (86.43%) was obtained at 2 M KOH, indicating that moderate alkaline treatment effectively enhanced silica purity while preserving the integrity of the silica framework. At this concentration, KOH promoted surface activation and impurity removal without causing substantial degradation of the siloxane network. However, further increases in KOH concentration resulted in a sharp decline in SiO_2 content, reaching 36.56% at 5 M KOH. This behavior suggests that excessive alkaline conditions induced partial dissolution of the silica structure through cleavage of Si–O–Si bonds, thereby destabilizing the pore framework and reducing silica stability (Umeda and Kondoh, 2010).

Table 3. Analysis of compound in the adsorbent at various KOH concentrations

Compound (%)	KOH concentration				
	1M	2M	3M	4M	5M
SiO_2	58.614	86.434	62.978	38.848	36.559
MgO	5.862	1.857	3.822	2.802	3.689
K_2O	14.347	11.004	14.100	35.132	43.414
CaO	12.229	2.148	6.982	3.407	4.477
Al_2O_3	1.304	1.323	1.096	7.265	1.228

In contrast, the K_2O content increased progressively with increasing KOH concentration, reaching a maximum value of 43.41% at 5 M KOH. The incorporation of potassium species into the silica framework enhances surface basicity and increases the number of active adsorption sites available for CO_2 capture. Potassium-containing species can facilitate stronger interactions between the adsorbent surface and acidic CO_2 molecules through chemisorption mechanisms involving carbonate formation (Zunigal et al., 2016). Furthermore, alkaline impregnation may improve pore accessibility and gas diffusion by modifying the pore structure of the adsorbent (Fouda-Mbanga et al., 2024). Nevertheless, excessive KOH loading may simultaneously induce over-activation, resulting in structural deterioration, partial pore collapse, and loss of structural order within the silica matrix. Similar observations were reported by Oginni et al. (2019), who found that excessive alkaline activation can negatively affect adsorption performance due to severe framework degradation.

The concentrations of MgO, CaO, and Al_2O_3 also exhibited fluctuating trends with increasing KOH concentration. The gradual reduction in MgO and CaO contents suggests partial dissolution and migration of metal species under highly alkaline conditions, while the decrease in Al_2O_3 indicates hydrolysis of aluminosilicate structures caused by hydroxide attack on Al–O–Si bonds, which are less stable than Si–O–Si linkages (Manurung et al., 2023). Overall, these findings indicate that KOH impregnation exerts a dual effect on the adsorbent structure by enhancing surface basicity and potassium incorporation while simultaneously risking structural degradation at excessive concentrations. Therefore, optimization of KOH concentration is essential to balance the beneficial increase in active basic sites with the preservation of silica structural integrity, ultimately maximizing CO_2 adsorption performance.

Morphological and structural characterization

The surface morphology of silica synthesized using different citric acid concentrations was analyzed using Scanning Electron Microscopy (SEM), as shown in Figure 4. In general, all samples exhibited irregular spherical particles with rough and heterogeneous surfaces, indicating the formation of porous silica structures during calcination and acid purification. Similar morphologies have also been reported by Pa et al. (2016) and Manurung et al. (2023).

At lower citric acid concentrations (1–2%), the silica surfaces appeared rough and compact

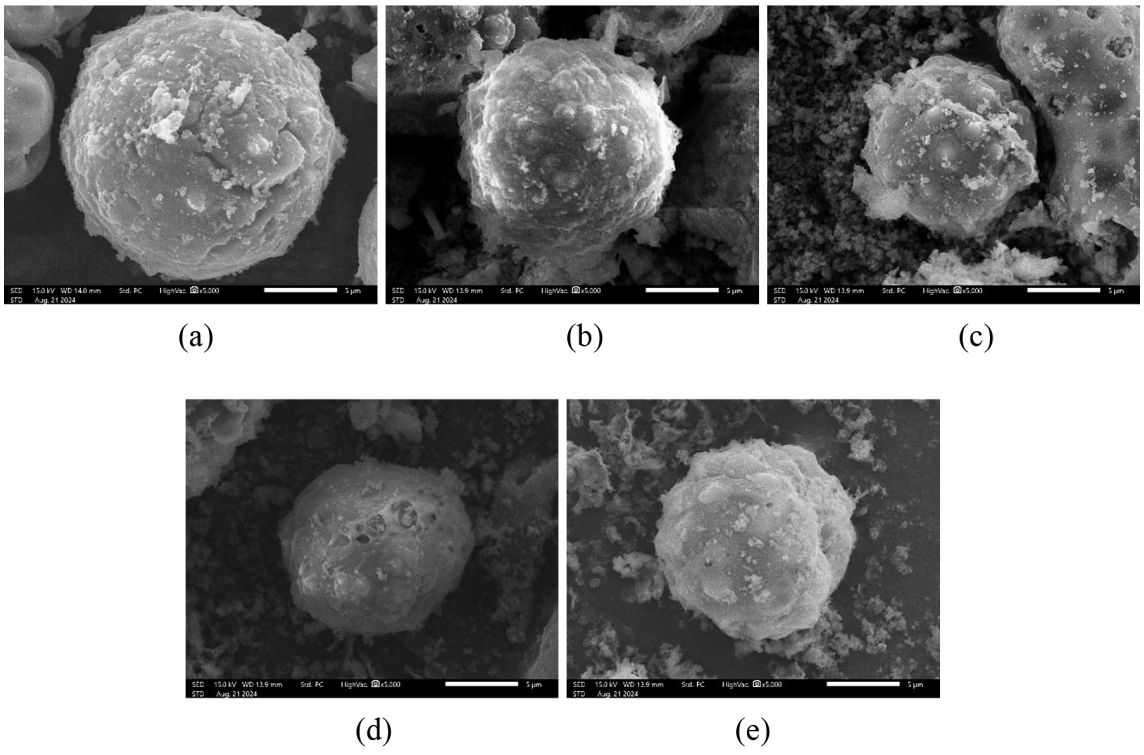

Figure 4. Morphology of silica at different citric acid concentrations: (a) 1%, (b) 2%, (c) 3%, (d) 4%, and (e) 5%

with visible agglomerated impurities, suggesting incomplete removal of inorganic compounds such as Ca and Mg oxides. Limited pore development was also observed, indicating restricted accessibility of the internal structure. Increasing the citric acid concentration to 3–4% resulted in cleaner and more homogeneous surfaces with more visible pores and cavities, indicating more effective impurity removal through the chelating action of citric acid. Among all samples, silica treated with 4% citric acid showed the most uniform morphology and pore distribution, consistent with the EDX results that indicated the highest Si purity (95.6%) and lowest Ca content. However, at 5% citric acid, slight surface deterioration and irregular deposits reappeared, suggesting excessive acid attack on the silica framework. This condition may cause partial dissolution of Si–O–Si bonds and reprecipitation of dissolved metal species, leading to reduced structural stability.

Overall, the SEM results demonstrate that citric acid concentration strongly affects the morphology and surface characteristics of silica synthesized from palm oil boiler ash. The 4% citric acid treatment produced the most favorable morphology with cleaner surfaces, better pore accessibility, and minimal structural damage, making it suitable for subsequent KOH impregnation and CO_2 adsorption applications.

Figure 5 presents the XRD analysis results of silica synthesized using a 4% citric acid concentration. The XRD pattern of the synthesized silica-based adsorbent reveals several diffraction peaks corresponding to crystalline silica phases. A prominent diffraction peak observed at approximately $2\theta \approx 21–22°$ and 26° indicates the presence of cristobalite and tridymite silica phases, confirming the crystalline nature of the synthesized material. Additional diffraction peaks detected around $2\theta \approx 31°$, 36°, and 48° further support the existence of silica-related crystalline structures within the adsorbent matrix. The broadening of several peaks and the elevated background intensity suggest that the material also contains a partially amorphous silica phase, which is commonly observed in silica derived from biomass ash. These findings are consistent with the study reported by Pa et al. (2016), in which X-ray diffraction analysis demonstrated that silica derived from palm ash predominantly exhibits a crystalline structure. The dominant silica peaks indicate that the purification and calcination processes successfully enhanced the silica content in the palm oil boiler ash. Furthermore, the relatively sharp diffraction peak near 22° demonstrates improved crystallinity after thermal treatment at 700 °C. The formation of crystalline silica structures may contribute to enhanced thermal stability and structural integrity of the adsorbent during the adsorption process.

Functional group analysis

FTIR analysis was performed on the adsorbent synthesized using 5 M KOH to investigate the surface functional groups and chemical interactions within the modified silica structure. As shown in Figure 6, the FTIR spectrum revealed characteristic absorption bands associated with silica and potassium-modified silica frameworks. The observed absorption peak is attributed to the interaction of K^+ species with the silica network, resulting in the formation of Si–O–K. The presence of these bonds confirms the successful incorporation of potassium species into the silica framework during the impregnation process. Such chemical modification is particularly important because the introduction of potassium-containing functional groups enhances the surface basicity and reactivity of the adsorbent, thereby improving its affinity toward acidic CO_2 molecules and promoting adsorption performance.

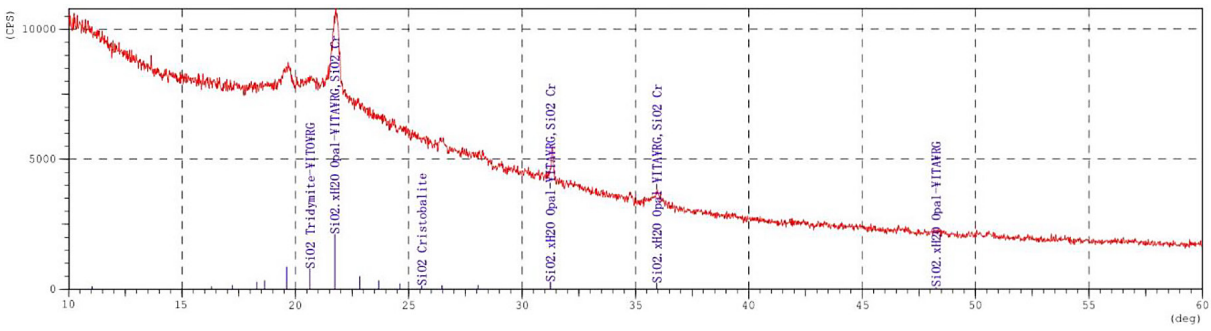

Figure 5. XRD pattern of silica synthesized using 4% citric acid

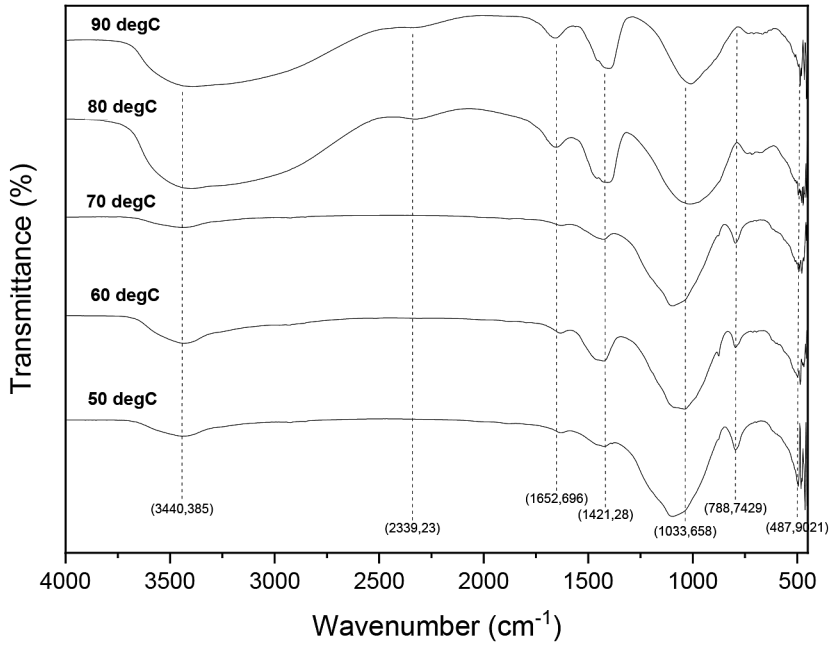

Figure 6. FTIR analysis of the adsorbent at varying impregnation temperatures

The Fourier Transform Infrared (FTIR) spectra of the KOH-impregnated boiler ash adsorbents exhibited several characteristic absorption bands corresponding to the functional groups present within the modified silica framework. The spectra obtained at different impregnation temperatures (50–90 °C) revealed absorption peaks in the range of 3440.38–487.90 cm^{-1}, indicating significant changes in surface chemistry following alkaline modification. A broad and intense absorption band observed at approximately 3440.38 cm^{-1} was attributed to O–H stretching vibrations associated with surface hydroxyl groups and adsorbed moisture, while the band near 2339.23 cm^{-1} corresponded to C–H stretching vibrations. The absorption peak at 1379 cm^{-1} was assigned to C–C bond vibrations, whereas the band at 1033.66 cm^{-1} indicated the presence of C–O stretching associated with alcohol or siloxane-related functional groups. Furthermore, the absorption peak located at 1421.28 cm^{-1} was attributed to the asymmetric stretching vibration of carbonate (CO_3^{2-}) species, suggesting interactions between potassium-containing sites and atmospheric or adsorbed CO_2 molecules.

Notably, the absorption band detected at approximately 788.74 cm^{-1} was associated with Si–O–K or potassium-related bonds formed during KOH impregnation, confirming the successful incorporation of potassium species into the adsorbent framework. The intensity of these absorption peaks increased with increasing impregnation temperature, indicating enhanced interaction between KOH and the silica surface at elevated temperatures. Among all samples, the adsorbent impregnated at 80 °C exhibited the highest potassium-related peak intensity, suggesting that this temperature provided the most favorable condition for potassium incorporation and surface activation. Enhanced potassium incorporation is expected to increase surface basicity and generate additional active sites for CO_2 adsorption, thereby improving adsorption performance (Taslim et al., 2019; Manurung et al., 2023).

Overall, the FTIR results demonstrate that controlled KOH impregnation significantly alters the chemical structure and functional group distribution of the silica-based adsorbent. The formation of potassium-containing functional groups, together with the increased intensity of hydroxyl and carbonate-related bands, confirms the successful surface modification of the adsorbent and highlights the important role of impregnation temperature in optimizing adsorbent properties for CO_2 capture applications.

Surface area analysis

The specific surface area and pore characteristics of the adsorbent were analyzed using the BET–BJH method. The analysis was performed on the adsorbent synthesized under the optimum conditions of 4 wt.% citric acid purification and 5 M KOH impregnation. The detailed BET–BJH results are presented in Table 4.

Table 4. Specific surface area and pore size distribution of the adsorbent

Parameter	Value	Unit
Surface area (BET)	0.24445	m^2/g
Total volume pore	0.0084633	cm^3/g
Average pore diameter (BJH)	14.089	nm
Median pore diameter (BJH)	3.8525	nm

BET–BJH analysis was conducted to evaluate the textural properties and pore structure of the synthesized adsorbent. The results showed that the adsorbent possessed a specific surface area of 0.24445 m^2/g, which is relatively low compared with conventional porous adsorbents that typically exhibit surface areas in the range of 100–1000 m^2/g. This relatively low surface area may be attributed to prolonged sample handling during the analysis, which potentially allowed adsorption of moisture from the surrounding atmosphere onto the adsorbent surface, thereby partially blocking accessible pores and reducing the measured surface area.

Despite the low BET surface area, the BJH pore size distribution analysis revealed an average pore diameter of 14.089 nm and a median pore diameter of 3.8525 nm, indicating the presence of a mesoporous structure. According to the IUPAC classification, materials with pore diameters between 2 and 50 nm are categorized as mesoporous. This observation is further supported by the nitrogen adsorption–desorption isotherm shown in Figure 7, which exhibits a Type IV isotherm accompanied by a distinct hysteresis loop at relative pressures (P/P_0) of 0.9–1.0. Such behavior is characteristic of mesoporous materials and indicates multilayer adsorption within the pore network.

The mesoporous characteristics of the adsorbent are particularly beneficial for CO_2 adsorption because mesopores facilitate efficient gas diffusion and improve accessibility of CO_2 molecules to active adsorption sites. In addition, the relatively narrow pore size distribution enhances molecular transport and adsorption interactions within the pore structure. Previous studies have reported that mesoporous adsorbents generally exhibit favorable CO_2 adsorption performance due to the balance between pore accessibility and diffusion efficiency (Samanta et al., 2012). Despite the relatively low specific surface area and pore volume, the mesoporous structure of the adsorbent demonstrates promising potential for CO_2 capture applications. Further enhancement through surface activation or impregnation with active materials

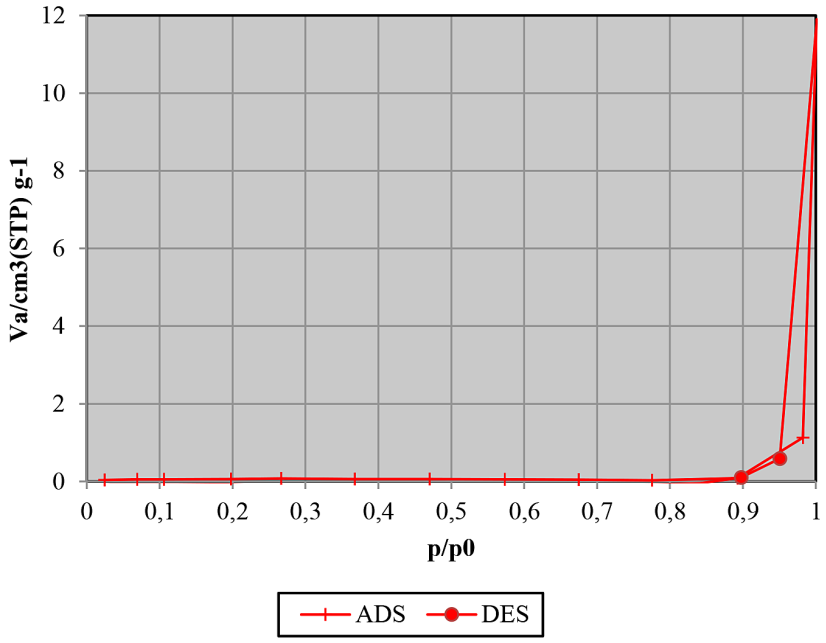

Figure 7. Nitrogen adsorption–desorption isotherm of the silica–potassium adsorbent

may further improve the adsorption performance by increasing the number of accessible active sites and strengthening interactions between the adsorbent surface and CO_2 molecules.

CO_2 adsorption kinetics and adsorption capacity analysis

Kinetic analysis was conducted to evaluate the adsorption rate and mechanism of the KOH-impregnated silica adsorbents at different impregnation temperatures. The experimental data were analyzed using pseudo-first-order and pseudo-second-order kinetic models. The calculated kinetic parameters, presented in Table 5, provide insights into the adsorption behavior and the effect of impregnation temperature on the adsorption performance of the adsorbents.

The kinetic parameters calculated from the pseudo-first-order and pseudo-second-order models are presented in Table 5. The pseudo-first-order rate constant (k_1) exhibited relatively low values with no consistent trend as the impregnation temperature increased, indicating that this model was insufficient to accurately describe the adsorption behavior of the synthesized adsorbent. In contrast, the pseudo-second-order rate constant (k_2) increased progressively with increasing impregnation temperature up to 80 °C, followed by a decline at higher temperatures. This trend suggests that moderate impregnation temperatures enhance the formation of active adsorption sites and improve adsorbent reactivity, whereas excessive temperatures may induce partial pore collapse or structural degradation of the adsorbent.

The correlation coefficient (R^2) further confirmed that the pseudo-second-order model provided a superior fit to the experimental data, with R^2 values approaching unity at all temperatures, while the pseudo-first-order model exhibited lower and more fluctuating R^2 values. These findings indicate that CO_2 adsorption onto the KOH-impregnated silica adsorbent is predominantly governed by chemisorption involving strong interactions between CO_2 molecules and potassium-containing active sites. The dominance of pseudo-second-order kinetics is consistent with the findings reported by Wang et al. (2022), who observed that KOH impregnation shifted the adsorption mechanism from physisorption-dominated behavior to chemisorption-controlled adsorption due to the presence of alkali metal species such as K_2O. The enhanced adsorption performance observed at 80 °C therefore indicates that this temperature represents the optimum impregnation condition for maximizing active site formation while preserving the structural integrity of the adsorbent.

Following the kinetic analysis, the equilibrium adsorption capacity of the adsorbent was evaluated to determine its overall CO_2 adsorption performance. The equilibrium adsorption capacities obtained under different operating conditions are summarized in Table 6.

Adsorption capacity tests were conducted on silica-based adsorbents impregnated with 5 M KOH at temperatures ranging from 70 to 110 °C. The adsorption performance, summarized in

Table 5. Adsorbent kinetic parameter

Kinetic model	Unit	Impregnation temperature (°C)				
		70	80	90	100	110
1st Pseudo-order	k_1 (sec^{-1})	1×10^{-6}	7×10^{-6}	9×10^{-8}	2×10^{-6}	2×10^{-7}
	R^2	0.1362	0.9101	0.0556	0.976	0.1773
2nd Pseudo-order	k_2 (g/mg.min)	0.01106	0.01353	0.01326	0.01030	0.00916
	R^2	1	1	1	1	1

Table 6. Adsorption capacity test data

KOH concentration (M)	Impregnation temperature (°C)	P_0 (atm)	P_e (atm)	C_e (mg/L)	q_e (mg/g)	Kapasitas adsorpstion capacities (mg/g)
5	70	4.944	4.532	7.842	1.797	61.25
5	80	4.964	3.991	6.905	3.398	144.80
5	90	4.964	4.210	7.261	3.202	112.11
5	100	4.954	4.295	7.431	2.876	98.04
5	110	4.944	4.357	7.588	2.707	87.30

Table 5, showed that the highest CO_2 adsorption capacity (144.8 mg/g) was achieved at an impregnation temperature of 80 °C. This result indicates that 80 °C provides the optimum condition for potassium incorporation, pore development, and active site formation within the silica framework. At higher temperatures, the adsorption capacity gradually decreased, likely due to excessive thermal activation causing partial pore collapse and structural degradation of the adsorbent.

The improved adsorption performance after KOH impregnation is attributed to the formation of potassium-containing active sites, particularly K_2O species, which enhance surface basicity and promote stronger chemisorption interactions with acidic CO_2 molecules. Although the adsorbent possesses a relatively low surface area, the high K_2O content contributes significantly to its adsorption capability by providing abundant active sites for CO_2 binding. In addition, the lower equilibrium CO_2 concentration (C_e) and C_e/q_e ratio observed at 80–90 °C indicate more efficient CO_2 uptake within this temperature range. surface functionalization significantly improves CO_2 adsorption due to the introduction of chemically active groups that strengthen adsorbate–surface interactions (Keramati and Ghoreyshi, 2014).

The present results are also consistent with the findings of Pattanshetti et al. (2025), who reported that KOH activation effectively engineered the pore structure and surface functionality of nanoporous activated carbon derived from waste floral foam, resulting in enhanced CO_2 adsorption capacity. Likewise, Tumurbaatar et al. (2023) demonstrated that surface modification of mesoporous SBA-15 silica significantly improved CO_2 adsorption performance due to enhanced surface reactivity and active site availability. Overall, these findings confirm that controlled KOH impregnation plays a critical role in optimizing the physicochemical properties of silica-based adsorbents and enhancing their potential for CO_2 capture applications.

CONCLUSIONS

The adsorption capacity tests demonstrated that silica-based adsorbents impregnated with 5 M KOH exhibited the highest CO_2 adsorption capacity of 144.8 mg/g at an impregnation temperature of 80 °C. This result suggests that the selected impregnation condition effectively enhanced potassium incorporation, surface basicity, and the formation of active adsorption sites within the silica framework. At higher temperatures, the adsorption capacity gradually decreased, likely due to excessive thermal activation that induced partial pore collapse and structural degradation of the adsorbent.

The enhanced adsorption performance after KOH impregnation is primarily attributed to the presence of potassium-containing active species, particularly K_2O, which promote stronger chemisorption interactions with acidic CO_2 molecules. The dominance of pseudo-second-order kinetics further supports the contribution of chemisorption mechanisms in the adsorption process. Although the adsorbent exhibited a relatively low BET surface area, the mesoporous structure and high potassium loading, with the silica–potassium adsorbent containing approximately 43% K_2O due to the use of 5 M KOH concentration during impregnation, likely facilitated CO_2 diffusion and increased the availability of chemically active sites for adsorption. Therefore, the adsorption behavior observed in this study appears to be governed more strongly by surface chemical interactions than by physical adsorption associated with high surface area alone.

Nevertheless, the relatively high CO_2 adsorption capacity compared with the low measured surface area suggests that additional mechanisms may contribute to the overall adsorption process. Possible factors include localized chemisorption on potassium-rich active sites, the formation of carbonate species, and the presence of accessible mesoporous channels that facilitate CO_2 transport within the adsorbent structure. However, further investigation using advanced surface characterization techniques and detailed adsorption mechanism studies is still required to fully elucidate the relationship between potassium incorporation, pore structure, and adsorption performance. Future studies are also recommended to investigate in greater detail the respective contributions of chemisorption and physisorption during CO_2 uptake, including the identification of reaction pathways, carbonate formation mechanisms, and the role of pore structure in facilitating gas diffusion and adsorption interactions. Overall, the results indicate that controlled KOH impregnation significantly improves the physicochemical properties and CO_2 adsorption potential of silica-based adsorbents derived from palm oil boiler ash.

Acknowledgement

This research is funded by USU for the 2024 fiscal year according to research contract number: 18589/UN5.1.R/PPM/2024, dated May 30, 2024

REFERENCES

1. Ajiz, H. A., Widiyastuti, W., Setyawan, H., Nurtono, T., Suari, N. M. I. P., Qomariyah, L., Budhi, Y. W., & Suherman, S. (2025). Direct surface modification of a silica-based adsorbent for CO_2 capture from coir fibers dissolved in a sulfur-free alkali-urea system. *Advanced Powder Technology*, *36*(6), 104912. https://doi.org/10.1016/j.apt.2025.104912
2. Boonchuay, A. and Worathanakul, P. (2022). The diffusion behavior of CO_2 adsorption from a CO_2/N_2 gas mixture on zeolite 5A in a fixed-bed column. Atmosphere 2022, 13, 513. https://doi.org/10.3390/atmos13040513
3. Cahyono, W. E., Parikesit, Joy, B., Setyawati, W., & Mahdi, R. (2022). Projection of CO_2 emissions in Indonesia. *Materials Today: Proceedings, 63*, S438–S444. https://doi.org/10.1016/j.matpr.2022.04.091
4. Cho, A. R., Won, Y., Nam, H., Park, J., Jo, S.-H., Kim, J.-Y., Park, Y. C., Bae, Y.-S., & Lee, Y.-R. (2026). Shaping spherical porous carbon beads impregnated with K_2CO_3 for CO_2 capture in humid flue gases and indoor air with low pressure drop. *Separation and Purification Technology*, *389*, 136930. https://doi.org/10.1016/j.seppur.2026.136930
5. de Castro-Alves, L., Yáñez-Vilar, S., González-Goméz, M. A., Garcia-Acevedo, P., Arnosa-Prieto, Á., Piñeiro-Redondo, Y., & Rivas, J. (2024). Understanding adsorption mechanisms and metal ion selectivity of superparamagnetic beads with mesoporous CMK-3 carbon and commercial activated carbon. *Microporous and Mesoporous Materials*, *374*, 113159. https://doi.org/10.1016/j.micromeso.2024.113159
6. Dias, E. A. P., da Silva, D. G., Amaral, M. C., Pereira, L. dos S., de Melo, D. C., & Vasconcelos, W. L. (2026). CO_2 adsorption by zeolites: State-of-the-art, techniques, and emerging trends. *Microporous and Mesoporous Materials*, *400*, 113904. https://doi.org/10.1016/j.micromeso.2025.113904
7. Dziejarski, B., Serafin, J., Andersson, K., & Krzyżyńska, R. (2023). CO_2 capture materials: a review of current trends and future challenges. *Materials Today Sustainability*, 100483.
8. Fouda-Mbanga, B. G., Velempini, T., Pillay, K., & Tywabi-Ngeva, Z. (2024). Heavy metals removals from wastewater and reuse of the metal-loaded adsorbents in various applications: A review. *Hybrid Advances*, *6*, 100193. https://doi.org/10.1016/j.hybadv.2024.100193
9. Francy, A., Ragi, T. M., Mohamed, A. P., & Solaiappan, A. (2025). CO_2 adsorption studies of hydrophobic silica sorbent functionalized with silicone oil-amine blends under low-temperature conditions. *ACS Applied Engineering Materials*, *3*(6), 1905–1914. https://doi.org/10.1021/acsaenm.5c00365
10. Gunawardene, O. H., Gunathilake, C. A., Vikrant, K., & Amaraweera, S. M. (2022). Carbon dioxide capture through physical and chemical adsorption using porous carbon materials: A review. *Atmosphere*, *13*(3), 397.
11. Hui, Q., Fu, J., Xu, H., Wang, C., Ding, Q., Zhu, W., Sun, J., Zhou, Z., Wu, Y., Hu, X., & Zhang, Z. (2025). Metal–organic frameworks for CO_2 capture: Challenges and efforts from laboratory research to industrial applications. *Industrial & Engineering Chemistry Research*, *64*(19). https://pubs.acs.org/doi/10.1021/acs.iecr.4c04997
12. Keramati, dan Ghoreysi M., Ashgar A. (2014). Improving CO_2 adsorption onto activated carbon through functionalization by chitosan and triethylenetetramine. *Physica E: Low-dimensional Systems and Nanostructures* 57, March, 161-168.
13. Kupgan, Grit.; Lauren J. Abbott.; Kyle E. Hart.; dan Coray M. Colina. (2018). Modeling amorphous microporous polymers for CO_2 capture and separations. *ACS Publication: Chemical Reviews*, 118, hal. 5488-5538. DOI: 10.1021/acs.chemrev.7b00691
14. Li, C., Zhang, X., Yin, Y., Xi, F., Wang, S., Hu, Q., Wang, J., & Bing, L. (2025). The mechanism of citric acid and oxalic acid on dissolution of high-silicon iron tailings. *Journal of Industrial and Engineering Chemistry*, *143*, 319–326. https://doi.org/10.1016/j.jiec.2024.08.034
15. Manurung, R., Parinduri, S. Z. D. M., Hasibuan, R., Tarigan, B. H., & Siregar, A. G. A. (2023). Synthesis of nano-CaO catalyst with SiO_2 matrix based on palm shell ash as catalyst support for one cycle developed in the palm biodiesel process. *Case Studies in Chemical and Environmental Engineering*, *7*, 100345. https://doi.org/10.1016/j.cscee.2023.100345
16. Misran, E., Bani, O., Dina, S. F., Harahap, R., & Wahyuni, N. (2019). Characterization of coal fly ash based adsorbent for CO_2 removal. *Journal of Physics: Conference Series*, *1230*, 012042. https://doi.org/10.1088/1742-6596/1230/1/012042
17. Mohammad, Karbalaei N., Ghaemi, A., Tahvildari, K. and Sharif, A. A. M. (2020). Experimental Investigation and Modeling of CO2 Adsorption Using Modified Activated Carbon. *Iranian Journal of Chemistry and Chemical Engineering*, *39*(1), 177-192. https://doi.org/10.30492/ijcce.2020.37648
18. Oginni, O., Singh, K., Oporto, G., Dawson-Andoh, B., McDonald, L., & Sabolsky, E. (2019). Influence

of one-step and two-step KOH activation on activated carbon characteristics. *Bioresource Technology Reports*, *7*, 100266. https://doi.org/10.1016/j.biteb.2019.100266

19. Pa, F. C., Abdullah, C., & Bari, M. F. (2016). Palm ash as an alternative source for silica production. *MATEC Web of Conferences, 78*, Article 01062. https://doi.org/10.1051/matecconf/20167801062
20. Pattanshetti, A., Jadhav, V., Koli, A., Kwiatkowski, M., Motkuri, R. K., Kim, D.-K., & Sabale, S. (2025). Waste floral foam to nanoporous activated carbon for efficient CO_2 capture: An investigation on the property-performance correlation of KOH impregnation. *Waste Management Bulletin*, *3*(1), 234–242. https://doi.org/10.1016/j.wmb.2025.01.007
21. Penchah, Ramezanipour H.; Gilani H.G..; dan Ahad G. (2020). CO_2, N_2, and H_2 adsorption by hypercross-linked polymers and gas their selectivity evaluation by solid equilibrium. *ACS Publication: Journal of Chemical & Engineering Data*. https://dx.doi.org/10.1021/acs.jced.0c00541
22. Putri, A. M. H., Ramadhoni, B. F., Yuzir, M. A. M., Riyadi, F. A., & Muharam, Y. (2026). Activated carbon from tea twig waste via KOH activation and carbonization by conventional furnace or ultrafast arc plasma for CO_2 capture. *Chemical Engineering Journal Advances*, *26*, 101096. https://doi.org/10.1016/j.ceja.2026.101096
23. Samanta, A., Zhao, A., Shimizu, G. K. H., Sarkar, P., & Gupta, R. (2012). Post-combustion CO_2 capture using solid sorbents: A review. *Industrial & Engineering Chemistry Research*, *51*(4), 1438–1463. https://pubs.acs.org/doi/10.1021/ie200686q
24. Sathishkumar, R., & Prakash, R. (2026). A review on activated carbons (AC) for CO_2 capture applications: Preparation, characterisation, and surface modification methods. *Fuel* 405, Part B, https://doi.org/10.1016/j.fuel.2025.136521
25. Sattari, A.; Ramazani A.; Aghahosseini H.; Aroua M.K. (2021). The application of polymer containing materials in CO_2 capturing via absorption and adsorption methods.
26. Novi S., Fitriani, Dewi R., Mulyawan R., A. Muslim A., Husin H.,Yunardi, dan Mutia R. (2021). Characterization of bottom ash waste adsorbent from palm oil plant boiler burning process to adsorb carbon dioxide in a fixed bed column. *Indones. J. Chem.*, 2021, 21 (6), 1454 – 1462. https://doi.org/10.22146/ijc.66509
27. Taslim, I., Bani, O., Parinduri, S. Z. D. M., Ningsih, P. R. W., & Taruna, N. (2019). Preparation, characterization, and application of natural zeolite from Tapanuli, Indonesia, modified with KOH as catalyst support for transesterification of rice bran oil. *International Journal of Engineering Research and Technology*, *12*(9), 1452–1456.
28. Tumurbaatar, O., Popova, M., Mitova, V., Shestakova, P., & Koseva, N. (2023). Engineering of silica mesoporous materials for CO_2 adsorption. *Materials*, *16*(11), 4179. https://doi.org/10.3390/ma16114179
29. Umeda, J., & Kondoh, K. (2010). High-purification of amorphous silica originated from rice husks by combination of polysaccharide hydrolysis and metallic impurities removal. *Industrial Crops and Products*, *32*(3), 539-544. https://doi.org/10.1016/j.indcrop.2010.07.002
30. Wang, Q., Luo, J., Zhong, Z., & Borgna, A. (2011). CO_2 capture by solid adsorbents and their applications: Current status and new trends. *Energy & Environmental Science*, *4*(1), 42–55. https://pubs.rsc.org/en/content/articlelanding/2011/ee/c0ee00064g
31. Wang, S., Lee, Y.-R., Won, Y., Kim, H., Jeong, S.-E., Hwang, B. W., Cho, A. R., Kim, J.-Y., Park, Y. C., Nam, H., Lee, D.-H., Kim, H., & Jo, S.-H. (2022). Development of high-performance adsorbent using KOH-impregnated rice husk-based activated carbon for indoor CO_2 adsorption. *Chemical Engineering Journal*, *437*(Part 1), 135378. https://doi.org/10.1016/j.cej.2022.135378
32. Wardhani, G. A. P. K., Nurlela, & Azizah, M. (2017). Silica content and structure from corncob ash with various acid treatment (HCl, HBr, and citric acid). *Molekul*, *12*(2), 174–181. https://doi.org/10.20884/1.jm.2017.12.2.382
33. Zúñiga, Sebastián Lira., César Sáez-Navarrete1, Leonardo Rodríguez-Córdova, Leandro Herrera-Zeppelin, Ronaldo Herrera-Urbina. (2016). CO_2 Adsorption On Agricultural Biomass Combustion Ashes. Maderas. *Ciencia y tecnología* 18(4): 607-616, 2016. https://doi.org/10.4067/S0718-221X2016005000053.